INTERNATIONAL STANDARD

ISO 16413

First edition
2013-02-15

Evaluation of thickness, density and interface width of thin films by X-ray reflectometry — Instrumental requirements, alignment and positioning, data collection, data analysis and reporting

Évaluation de l'épaisseur, de la densité et de la largeur de l'interface des films fins par réflectométrie de rayons X — Exigences instrumentales, alignement et positionnement, rassemblement des données, analyse des données et rapport

Reference number
ISO 16413:2013(E)

COPYRIGHT PROTECTED DOCUMENT

ISO copyright office
Case postale 56 • CH-1211 Geneva 20
Tel. + 41 22 749 01 11
Fax + 41 22 749 09 47
E-mail copyright@iso.org
Web www.iso.org

Published in Switzerland

Contents

Page

Foreword

ISO (the International Organization for Standardization) is a worldwide federation of national standards bodies (ISO member bodies). The work of preparing International Standards is normally carried out through ISO technical committees. Each member body interested in a subject for which a technical committee has been established has the right to be represented on that committee. International organizations, governmental and non-governmental, in liaison with ISO, also take part in the work. ISO collaborates closely with the International Electrotechnical Commission (IEC) on all matters of electrotechnical standardization.

International Standards are drafted in accordance with the rules given in the ISO/IEC Directives, Part 2.

The main task of technical committees is to prepare International Standards. Draft International Standards adopted by the technical committees are circulated to the member bodies for voting. Publication as an International Standard requires approval by at least 75 % of the member bodies casting a vote.

Attention is drawn to the possibility that some of the elements of this document may be the subject of patent rights. ISO shall not be held responsible for identifying any or all such patent rights.

ISO 16413 was prepared by Technical Committee ISO/TC 201, *Surface chemical analysis*.

Introduction

X-Ray Reflectometry (XRR) is widely applicable to the measurement of thickness, density and interface width of single layer and multilayered thin films which have thicknesses between approximately 1 nm and 1 µm, on flat substrates, provided that the layer, equipment and X-ray wavelength are appropriate. Interface width is a general term; it is typically composed of interface or surface roughness and/or density grading across an interface. The specimen needs to be laterally uniform under the footprint of the X-ray beam. In contrast with typical surface chemical analysis methods which provide information of the amount of substance and need conversion to estimate thicknesses, XRR provides thicknesses directly traceable to the unit of length. XRR is very powerful method to measure the thickness of thin film with SI traceability.

The key requirements for equipment suitable for collecting specular X-ray reflectivity data of high quality, and the requirements for specimen alignment and positioning so that useful, accurate measurements may be obtained are described in Clause 3.

The key issues for data collection to obtain specular X-ray reflectivity data of high quality, suitable for data treatment and modelling are described in Clause 4. The collection of the data is traditionally conducted by running single measurements under direct operator data input. However, recently data are often collected by instructing the instrument to operate in multiple runs. In addition to the operator mode, data can be collected making use of automated scripts, when available in the software program controlling the instrument.

The principles for analysing specular XRR data in order to obtain physically meaningful material information about the specimen are described in Clause 5. While specular XRR fitting can be a complex process, it is possible to simplify the implementation for quality assurance applications to the extent where it can be transparent to the user. There are many software packages, both proprietary and non-proprietary available for simulation and fitting of XRR data. It is beyond the scope of this document to describe details of theories and algorithms. Where appropriate, references are given for the interested reader.

The information required when reporting on XRR experiments is listed in Clause 6. A brief review of the possible ways to present XRR data and results is given and, when more than one option is available, the preferred one is indicated.

This document is not a textbook, it is a standard for performing XRR measurements and analysis. For a full explanation of the technique, please consult appropriate references [e.g. D. Keith Bowen and Brian K. Tanner, “X-Ray Metrology in Semiconductor Manufacturing”, Taylor and Francis, London (2006); M. Tolan, “X-ray Reflectivity from Soft Matter Thin Films“, Springer Tracts in Modern Physics vol. 148 (1999); U. Pietsch, V. Holy and T. Baumbach, “High Resolution X-Ray Scattering from Thin Films to Lateral Nanostructures”, Springer (2004); J. Daillant and A. Gibaud, “X-ray and Neutron Reflectivity: Principles and Applications”, Springer (2009)].

Note that proprietary techniques are not described in this International Standard.

Safety aspects related to the use of X-ray equipment are not considered in this document. During the measurements, the adherence to relevant safety procedures as imposed by law are the responsibilities of the user.

Evaluation of thickness, density and interface width of thin films by X-ray reflectometry — Instrumental requirements, alignment and positioning, data collection, data analysis and reporting

1 Scope

This International Standard specifies a method for the evaluation of thickness, density and interface width of single layer and multilayered thin films which have thicknesses between approximately 1 nm and 1 µm, on flat substrates, by means of X-Ray Reflectometry (XRR).

This method uses a monochromatic, collimated beam, scanning either an angle or a scattering vector. Similar considerations apply to the case of a convergent beam with parallel data collection using a distributed detector or to scanning wavelength, but these methods are not described here. While mention is made of diffuse XRR, and the requirements for experiments are similar, this is not covered in the present document.

Measurements may be made on equipment of various configurations, from laboratory instruments to reflectometers at synchrotron radiation beamlines or automated systems used in industry.

Attention should be paid to an eventual instability of the layers over the duration of the data collection, which would cause a reduction in the accuracy of the measurement results. Since XRR, performed at a single wavelength, does not provide chemical information about the layers, attention should be paid to possible contamination or reactions at the specimen surface. The accuracy of results for the outmost layer is strongly influenced by any changes at the surface.

2 Terms, definitions, symbols and abbreviated terms

2.1 Terms and definitions

2.1.1
incidence angle
angle betwen the incident beam and the specimen surface

2.1.2
critical angle
θ_c
angle between the incident beam and the specimen surface, below which there is total external reflection of X-rays, and above which the X-ray beam penetrates below the surface of the specimen

Note 1 to entry: The critical angle for a given specimen material or structure can be found by using simulation software, or approximated from the formula $\theta_c \approx \sqrt{2\delta}$ where $1 - \delta$ is the real part of the complex X-ray refractive index $n = 1 - \delta - i\beta$.

2.1.3
specimen length
dimension of the specimen in the plane of the incident and reflected X-ray beams and in the plane of the specimen

2.1.4
specimen width
dimension of the specimen perpendicular to the plane of the incident and reflected X-ray beams and in the plane of the specimen

2.1.5
specimen height
Z
dimension (thickness) of the specimen perpendicular to the plane of the specimen

2.1.6
layer thickness
thickness of an individual layer on the substrate

2.1.7
beam footprint
area on the specimen irradiated by the X-ray

2.1.8
beam spill-off
effect of grazing incidence that involves the reduction of the measured reflected intensity when part of the incident beam is not intercepted by the specimen, so that the part spills off the specimen

2.1.9
instrument function
analytical function describing the effects of instrument and resolution on the observed scattered X-ray intensity

2.1.10
reciprocal space
representation of the physical specimen and X-rays where the distance plotted is proportional to the inverse of real-space distances, and angles correspond to real-space angles

2.1.11
wave vector
$\boldsymbol{k}$
vector in reciprocal space describing the incident or scattered X-ray beams

2.1.12
scattering vector
$\boldsymbol{q}$
vector in reciprocal space giving the difference between the scattered and incident wave vectors

2.1.13
dispersion plane
plane containing the source, detector, incident and specularly reflected X-ray beams

2.1.14
specular X-ray reflectivity
reflected X-ray signal detected at an angle with the specimen surface as the incident X-ray beam with the specimen surface: $2\theta/2 = \omega$

Note 1 to entry: The detected, scattered X-ray intensity is measured as a function of either ω or 2θ or q_z (usually presented against q_z or ω).

2.1.15
diffuse X-ray reflectivity
X-ray scatter arising from the imperfection of the specimen

2.1.16
fringe
one of the repeating maxima in reflectometry data which arise from interference of the X-ray waves

Note 1 to entry: Fringe periods are related to the thickness of a layer (or layers) of contrasting electron density. Multiple layers give rise to series of superposed interfering fringes.

2.1.17
fringe contrast
qualitative description of the height of a fringe between its minimum and its maximum

Note 1 to entry: The greater the difference between minimum and maximum, the greater the contrast is said to be.

2.1.18
electron density
ρ_e
electrons per unit volume

Note 1 to entry: XRR typically measures electron density in electrons per nm^3 or per $Å^3$.

Note 2 to entry: This can be calculated from mass density.

2.1.19
mass density
ρ
common density (mass per unit volume)

Note 1 to entry: It is measured in kg m^{-3} (or sometimes in g cm^{-3}).

2.1.20
absorption length
L_{abs}
distance over which the transmitted intensity falls to 1/e of the incident intensity

2.1.21
2theta
2Θ
angle of the detected X-ray beam with respect to the incident X-ray beam direction

2.1.22
omega
ω
angle between the incident X-ray beam and the specimen surface

2.1.23
phi
Φ
angle of rotation about the normal to the nominal surface of the specimen

2.1.24
chi
χ
angle of tilt of specimen about an axis in the plane of the specimen and in the plane of the incident X-ray beam, X-ray source and detector

2.1.25
X, Y, Z coordinate system
orthogonal coordinate system in which X is the direction in the plane of the specimen, parallel to the incident beam when $\phi = 0$; Y is the direction in the plane of the specimen, perpendicular to the incident beam when $\phi = 0$; and Z is the direction normal to the plane of the specimen

2.2 Symbols and abbreviated terms

2θ	2Theta, the angle of the detected X-ray beam with respect to the incident X-ray beam
ω	Omega, the angle between the incident X-ray beam and the specimen surface
ϕ	Phi, the angle of rotation about the normal to the nominal surface of the specimen
χ	Chi, the angle of tilt of specimen about an axis in the plane of the specimen and in the plane of the incident X-ray beam, X-ray source and detector
θ_c	Critical angle
λ	Wavelength of the incident X-ray beam
ρ	Mass density
ρ_e	Electron density
$\boldsymbol{k}$	Wave vector
$\boldsymbol{q}$	Scattering vector
q_z	Scalar magnitude of the component of the scattering vector in reciprocal space normal to the specimen surface (corrected or uncorrected for refraction). $q_z = 4\pi/\lambda \times \sin(\theta)$
σ	root mean square height of the scale-limited surface (according to ISO 25178-2) or interface width
L_{abs}	Absorption length in the specimen
XRR	X-Ray Reflectometry or X-Ray Reflectivity
Z	specimen height

3 Instrumental requirements, alignment and positioning guidelines

3.1 Instrumental requirements for the scanning method

3.1.1 Schematic diagrams

The principal requirements are on the beam size and beam positioning over the coaxial centres of rotation of specimen (ω) and detector (2θ) axes.

Figure 1 shows a diagram of a basic collimated beam, scanning configuration for an XRR experiment. The case of a convergent beam and distributed detector is not shown.

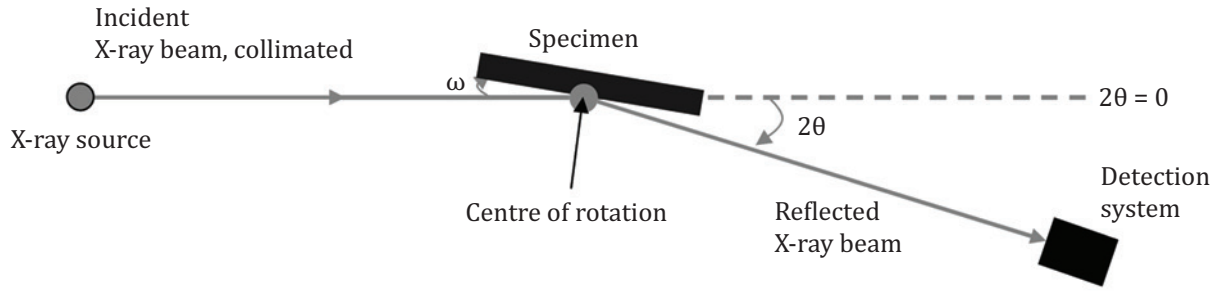

Key

ω angle between the specimen surface and the incident X-ray beam

2θ angle between the detected beam and 2θ = 0 (the extension of the incident X-ray beam)

NOTE The centre of rotation, where incident and reflected beams, the specimen surface and the rotation axes of ω and 2θ coincide, is highlighted as an orange disc.

Figure 1 — Schematic layout of a typical scanning XRR experimental configuration, projected into the plane of the source, detector, incident and specularly-reflected X-ray beams (the dispersion plane)

Figure 2 shows a schematic diagram of scanning configuration XRR in a three-dimensional view, indicating the diffuse scatter as well as the specularly reflected X-ray beam.

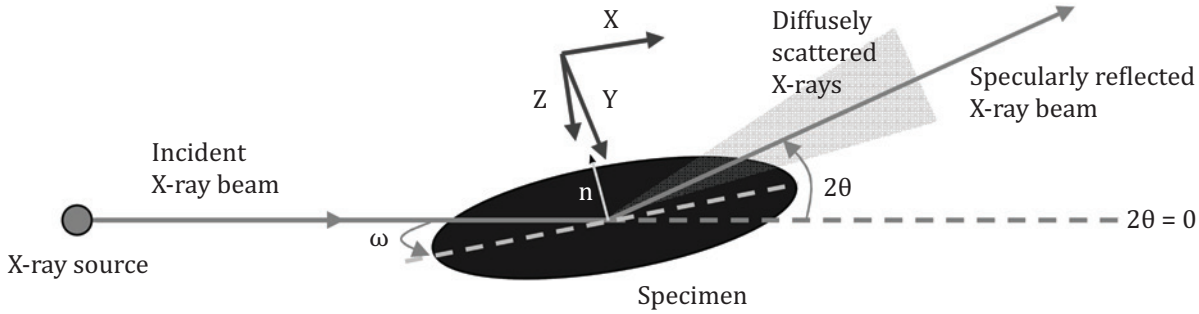

Key

ω angle between the specimen surface and the incident X-ray beam

2θ angle between the detected beam (at 2θ = 0) and whichever part of the reflected beam is of interest (the detected beam)

Figure 2 — Schematic diagram showing specular and diffusely reflected X-ray beams

3.1.2 Incident beam — Requirements and recommendations

3.1.2.1 Incident beam — Requirements

The following requirements shall apply to the collimated beam, scanning method. Similar considerations apply to the convergent beam, parallel data collection method.

a) The incident beam shall be stable (or can be compensated) within the time-frame of the experiment.

b) The incident beam shall be nominally monochromatic. The wavelength dispersion $d\lambda$ shall fulfil the following condition: $d\lambda < \lambda d\theta/\tan(\theta_m)$ where $d\theta$ is the beam divergence and θ_m is typically the maximum incidence angle where fringes are still observed.

EXAMPLE If using an incident beam of Cu Kα radiation (λ = 0,154 1 nm) with an angular divergence of 50 arc seconds, and if fringes are observed out to an incident angle of 3,5°, then $d\lambda$ needs to be less than 0,035 nm.

c) If the beam is not sufficiently collimated, the divergence of the beam limits the maximum detectable thickness. Practically, the maximum measurable thickness is less than $\lambda/6\sin(d\theta)$ where $d\theta$ is beam divergence for a suitable specimen. For typical laboratory equipment, the limit is a few hundred nm.

d) The incident intensity shall be such as to allow several orders of magnitude intensity range above background, since reflected intensity falls rapidly above the critical angle. Below the critical angle, there is total external reflection. Above the critical angle, reflected intensity falls at a rate proportional to q_z^{-4} for a perfectly smooth surface, and more rapidly than this for rough or/and graded surfaces.

3.1.2.2 Incident beam — Recommendations

The following recommendations concern the collimated beam, scanning method. Similar considerations concern the convergent beam, parallel data collection method.

a) The specimen should be laterally uniform under the area irradiated (the beam footprint) and observed by the detector. This may be achieved by control of incident and scattered beam slits and/or, for example, inserting a knife-edge near the specimen.

b) Beam spill-off should be minimized. This is especially important when the specimen angle is near and above the critical angle. The beam width compared to the specimen length should be such that there is no beam spill-off for a specimen angle which is above about 75 % (preferably less) of the critical angle. (See Figure 3.)

NOTE With the specimen parallel to the beam (ω = 0), the beam covers all of the specimen. The beam footprint varies with incident angle unless slits or knife-edge position are varied through the scan).

1) The maximum acceptable beam width for a given specimen size can then be found by geometry.

2) If there are very small specimens, it may not be practical to meet the recommended requirements. In this case, the accuracy and precision of densities and interface widths deduced may be compromised.

3) This is necessary so that the position of the critical angle can be ascertained with reasonable confidence, so that, if data analysis includes layer density and interface width parameters, these can be deduced with reasonable accuracy.

4) Some modelling and data fitting software allow the specimen size and beam size to be input, which allows data fitting where there is significant beam spill-off, but even so it is recommended that the specimen fill the incident beam from below the critical angle in order to have high confidence in fitting this region and obtaining good density information.

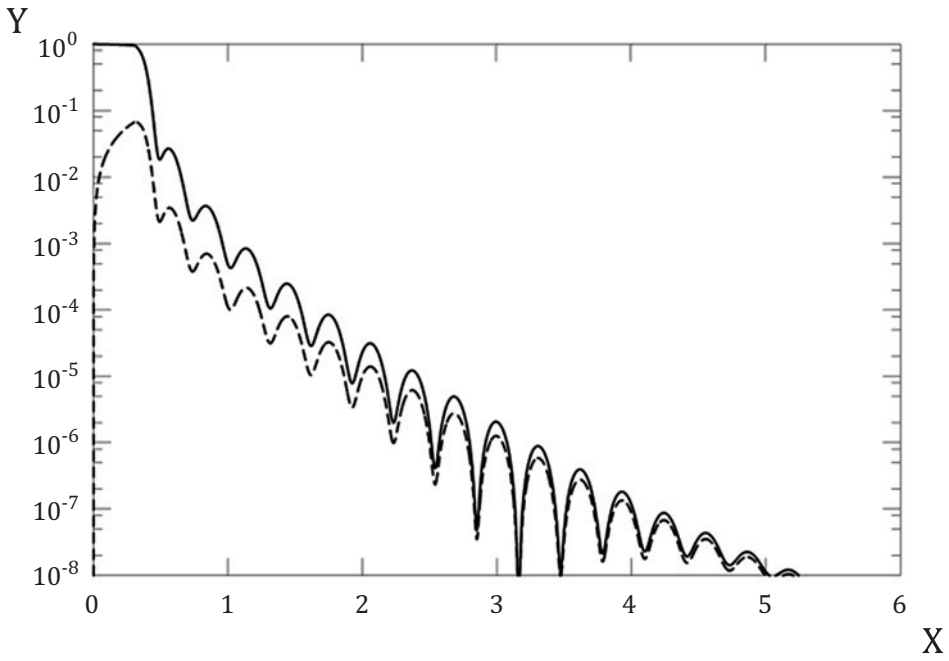

Key

X q_Z, in nm^{-1}

Y intensity, in a.u.

— simulated specular reflectivity of 20,0 nm Si_3N_4 (with 0,6 nm surface roughness) on bulk Si (with 0,3 nm interface width), without instrument function

--- simulated specular reflectivity of 20,0 nm Si_3N_4 (with 0,6 nm surface roughness) on bulk Si (with 0,3 nm interface width), with instrument function (0,5 mm source and detector slits and a 10 mm specimen)

NOTE The position of the critical angle for the small specimen is unclear and possibly apparently shifted, and the rate of decrease of reflected intensity with increasing specimen angle is affected. This affects the roughness or interface width deduced if the instrument function is not accurately taken into account in analysis. The positions of fringes are unaffected, so thickness analysis can proceed successfully.

Figure 3 — Simulated specular reflectivity of 20,0 nm Si_3N_4 on bulk Si, with and without instrument function

c) If the above recommended condition cannot be met, provided that spill-off does not continue much beyond the critical angle, fringes in the reflectometry data will still give an accurate measure of layer thicknesses.

d) That portion of the X-ray beam measured at the detector should not spill off the specimen perpendicular to the dispersion plane (the dispersion plane is perpendicular to the plane of Figure 1) in the case where measuring the direct beam intensity is used to align the specimen accurately over the centre of rotation of ω and 2θ.

3.1.3 Specimen — Requirements and recommendations

3.1.3.1 Specimen — Requirements

The following basic requirements shall be verified.

— XRR is a near-surface-sensitive technique. The specimen shall therefore be handled or treated only in such ways that the surface is not modified or that any modification is taken into account in the interpretation of the data. Modifications could include touching, mechanical or chemical polishing.

3.1.3.2 Specimen — Recommendations

The following basic recommendations should be followed.

a) The specimen should be laterally uniform under the beam footprint observed by the detector.

b) The specimen should fill the incident beam from a specimen angle significantly below the critical angle and for angles above this. It is recommended that the specimen should fill the beam from a maximum of 75 % of the critical angle.

c) The specimen should not be significantly bowed, or alignment precision and data quality are compromised. The effect of curvature can be minimized by minimizing the beam footprint on the specimen. It is recommended that the specimen should fill the beam from a maximum of 75 % of the critical angle. It may be possible to proceed with data analysis from curved specimens. Some data fitting models can take specimen curvature into account. Thickness values may be obtained with sufficient accuracy, but the accuracy of interface widths and density is poorer.

d) The specimen surface and interfaces (where applicable) should be smooth, with a root mean square (rms) roughness or interface width less than or similar to L_{abs}/θ_c. Refer to 5.2.1 for a more detailed description of roughness and interface width. Typically, this means $\sigma < 5$ nm maximum (above which, special models must be applied for the analysis) and preferably $\sigma < 3{,}5$ nm. Where the surface or interfaces are too rough, reflected intensity falls too rapidly with increasing specimen angle, and reflectometry data give no useful material information. Models used to fit data are also less reliable at very high interface widths.

3.1.4 Goniometer — Requirements

The following basic requirements shall be verified.

a) A mechanically well-aligned and stable X-ray goniometer is required.

b) For a scanning configuration, the ω and 2θ axes shall be capable of being moved such that intervals can be maintained in the ratio $\Delta(2\theta) = 2(\Delta\omega)$. Maintaining the ratio to one part in 1 000 is typically sufficient.

c) The intervals of ω and 2θ shall be capable of being small enough that at least five data points may be collected over a single thickness fringe. More data points are required for more complex specimens.

d) The specimen height (Z) shall be capable of being set accurately on the centre of rotation of ω and 2θ axes.

e) The specimen stage angle of tilt (χ) shall enable setting the specimen parallel to the incident beam slits.

3.1.5 Detector — Requirements

The following basic requirements shall be verified.

a) The detector response shall be stable within the time-frame of the experiment.

b) For the specular reflectivity data to be collected in a single scan, the angular resolution of the detector shall be such as to allow discrimination between the specular and diffuse reflectivity. It is

usual and recommended that the acceptance slits at the detector (where applicable) be set to match the incident beam width and divergence.

c) Either the detector shall be capable of linear (or linearized) response over the whole reflected intensity range (several orders of magnitude) or a system of calibrated attenuators to limit the detected intensity is required over appropriate parts of the data range in order that the detector can be linear (or linearized) in that range. Data in the different sections are then normalized using the attenuation factors.

NOTE For the requirements of specular reflectometry, as here, there is no discrimination in the plane perpendicular to the dispersion plane (i.e. in the plane perpendicular to the diagram in Figure 1). Reflected intensity is integrated in this direction.

3.2 Instrument alignment

Alignment checks may be part of automated routines available on particular equipment. Slit collimation of the scattered radiation is assumed. The following basic requirements shall be verified.

a) Set the X-ray source slit width to minimize spill off (typically 0,1 mm to 0,2 mm in a laboratory system).

b) Make sure that nothing unwanted obstructs the beam between the source and detector. The specimen and specimen mounting shall be out of the beam.

c) Start with the detector slits significantly wider than the source slits (many times wider).

d) The incident X-ray beam shall be accurately centred on the centre of rotation of the specimen and detector axes.

NOTE It is possible, with modern control software, that corrections to axes motions may take into account a non-ideal instrument alignment.

e) Set the detector slit width so that the acceptance angle is similar to the incident beam divergence. This typically means that the detector slit width is set the same as the source slit width in a laboratory system or about 20 % wider.

f) Scan the detector angle across the incident beam. The peak should be an approximately symmetric single maximum. Locate the position of the centre of the peak maximum (approximately at the centre of mass). Move the detector to this position to set the $2\theta = 0$ position accurately.

3.3 Specimen alignment

Equipment and its controls may include automatic specimen alignment, data collection and analysis routines, and may make use of other methods of alignment, e.g. range finders or position monitors. The procedure below describes one approach to specimen alignment relative to the X-ray beam in an aligned instrument.

a) The instrument shall be aligned correctly, with appropriate slit widths, with the incident beam accurately over the centre of rotation and the detector angle $2\theta = 0$ correctly set on the incident beam.

b) The angle, ω, between specimen surface and incident beam shall be calibrated so that zero sets the specimen surface approximately parallel to the incident beam.

c) If using a knife-edge, its position in Z, X, and tilt perpendicular to the beam direction (where available) shall be carefully set. This is done after adjusting the specimen position. The manufacturer's recommended operating instructions should be consulted.

d) Mount the specimen on the specimen stage, in a suitable and repeatable orientation as far as possible, e.g. notch or flat down, or cleaved edge parallel or perpendicular to the beam direction.

e) Where applicable, set the X-ray generator power to the manufacturer's recommended operating level. Ensure stable operation.

f) Move χ such that the specimen surface is nominally perpendicular to the plane containing the source, incident beam and detector.

g) Move the specimen to the X, Y, ϕ position required for the measurement. Make sure that nothing unwanted (such as the means of specimen mounting) can interfere with the incident or reflected beams.

h) Initially, make sure that Z is such that the incident beam initially passes unhindered past the specimen.

i) If required, insert an attenuator in the beam so that the detected intensity is well within the linear or linearized regime of the detector. Note the full beam intensity, I_{full}.

j) Move Z to move the specimen into the beam until about one quarter to one fifth of the full beam intensity is observed, i.e. move Z until $I_{observed} \sim I_{full}/4$ to $\sim I_{full}/5$.

k) Adjust ω until a maximum intensity is observed. If the maximum intensity is more than half the full beam intensity, go back to step (j).

l) Scan ω to find more precisely the position of maximum intensity. Set ω here.

m) Now set χ. Move Z until the incident beam is nearly eclipsed (to about 2 % of full beam intensity).

n) Scan χ both sides of the nominal position.

o) Set χ to the minimum of the scan profile.

p) Move Z until $I_{observed} = I_{full}/2$.

q) Scan ω again, and set ω at the intensity maximum, which should be $I_{full}/2$.

r) Make small adjustments in Z and ω if required until the maximum intensity on an ω scan is $I_{full}/2$. The specimen is now parallel to the incident beam and half way into it. Since the beam is over the centre of rotation of ω and 2θ, the surface of the specimen is now also over the centre of rotation.

s) It is standard practice on some XRR equipment to fit a knife-edge close to the specimen to define the beam and reduce scatter, although this is not essential on all equipment for obtaining high quality data. If a knife-edge is in use, it is set and adjusted at this point. Procedures are specific to the particular equipment configuration in use, and so are not discussed here.

t) Move 2θ to an angle significantly above the critical angle but such that there is sufficient intensity in the specularly reflected beam, i.e. well above the background level of the detector. Move ω to half 2θ.

NOTE In general, moving 2θ to ~0,5° to 1,0° (~1 800 to 3 600 arc sec) will be appropriate if using Cu Kα radiation or similar.

u) Reflected intensity is generally much weaker than the direct incident beam. Adjust or remove the attenuator (if applicable) in order that a clear intensity within the linear or linearized response of the detector is measurable. If the intensity is too low, decrease 2θ until a significant signal appears, but do not get too close to the critical angle.

v) Scan the ω axis over a sufficient range to see a clear peak as the specimen passes through the specular reflection condition. Then set ω to the point of highest intensity (Figure 4). This refines the specimen angle setting on a specular reflection, and is more precise than relying on setting the specimen surface parallel to the incident beam.

w) Go back to step p) and recheck the half beam position. If the half beam position changes, retract the knife edge (if used) and re-check the procedure from step p) onward.

x) The instrument may have an axis called ω - 2θ or θ - 2θ, in which case it may be helpful to recalibrate this axis to half the 2θ value. Or it may have an axis called 2θ - θ, in which case it may be helpful to recalibrate this at the 2θ value. However, the instrument controls may not permit this.

The specimen is now aligned and ready to scan.

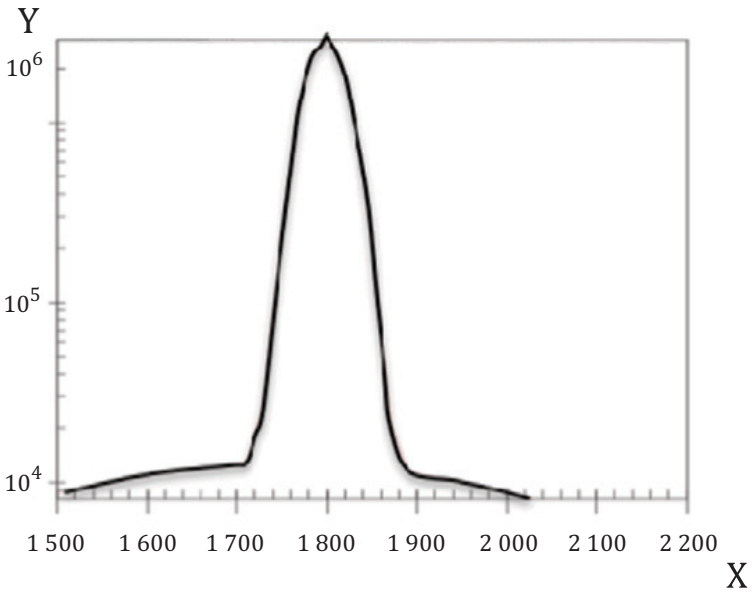

Key

X omega, in arc seconds

Y intensity, in cps

NOTE Since raw data are usually collected in angular units and a raw intensity scale, this figure is not shown as normalized intensity versus q_z.

Figure 4 — Scan of ω through the specular condition, with 2θ fixed at 3 600 arc seconds (1°)

4 Data collection and storage

4.1 Preliminary remarks

The X-ray generator shall be operating stably to the manufacturer's specification in an appropriate environment. Particular care shall be taken on switching on an X-ray generator, to allow a reasonable time to establish stable working conditions of electronics and X-ray beam. Refer to the manufacturer's start-up procedures.

4.2 Data scan parameters

For data collection, ω and 2θ angles are required to be moved or scanned. The specular angular condition ω = θ shall be fulfilled at each data collection point.

The scanning time is the time necessary to obtain the entire scan. Whenever possible, it is recommended to calculate, or at least estimate, the scanning time. This is particularly important when multiple scans or automated scripts are used for the data collection.

The collection time at each point may be kept fixed or variable (accumulated counts) (see 4.5).

4.3 Dynamic range

It is recommended that scans shall begin at ω = θ = 0° and end when reaching the background level. Following this recommendation will allow the best data analysis. However, to reduce scanning time, for particular requirements, limited range data scans can be collected.

A reliable alternative method to reduce the scanning time is the use of multiple scans for the data collection. Multiple scans allow the average of the data collected over different scans, taken at the same conditions, improving the statistics.

4.4 Step size (peak definition)

4.4.1 Fixed intervals scan

The intervals of ω and 2θ shall be capable of being small enough that at least five data points may be collected over a single thickness fringe. More data points are required for more complex specimens.

a) Five points on a fringe are sufficient for rapid analysis of a well-defined single-layer specimen where there is good fringe contrast.

b) Seven points is typically recommended over a single fringe. More data points may be collected if desired.

c) If the specimen structure has multiple layers giving overlapping and interfering fringes in the reflectometry data, more points per fringe may be required in order to define the shape accurately and so enable analysis to distinguish between multiple layers.

Scanning in step size at fixed intervals is rather common.

4.4.2 Continuous scan

Alternatively, instead of a scan in intervals with data collection at each point, ω and 2θ can be continuously moved at a constant speed, while the data are collected with a fixed sampling rate (sampling time).

The same conditions on points over fringe as in 4.4.1 shall be fulfilled also in the continuous scan approach.

This approach is recommended when a simple specimen structure is measured over a large dynamic range ($2\theta > 10°$) in the presence of a fast dynamic detector, because it optimizes the collection and scanning time.

4.5 Collection time (accumulated counts)

The collection time may be kept fixed or variable. The latter is also known as accumulated counts approach.

In the fixed collection time approach, each data point is collected over the same time interval.

In the accumulated counts approach, the collecting time at each data point is stopped when a threshold number of counts is achieved. In this case, an algorithm taking into account the detector dead time correction is used to re-normalize the collected data. Whenever possible, a mixed approach is recommended, where the maximum collection time is fixed and a threshold counts is considered. The threshold value shall be chosen to grant the linearity of the detector.

For example, because of the fast exponential decay of the specularly reflected intensity, when starting the data collection from 0°, in the initial part of the scan, a high count rate is registered, then the accumulated counts limit is a great advantage to reduce the total scanning time. On the contrary, far from the critical angle region, for high angles or with rough specimens, the fixed collection time approach is envisaged, otherwise the accumulated count limit would require much longer time to be achieved without any improvement in the signal to noise ratio.

4.6 Segmented data collection

It is recommended that, whenever possible, a single scan shall begin at $\omega = \theta = 0°$ and end when reaching the background level is acceptable to collect data in segment.

A segment, or limited range data scan, is intended as a partial scan over a limited region of the dynamic range which covers a limited angular range defined by an initial and a final angle specular condition.

It is recommended that at least one overlapping collected point exists for each segmented scan to proper allow the joint of the segmented scans and the re-construction of a full range scan.

4.7 Reduction of noise

In data collection, the number of counts follows a Poisson statistic. Controlling the count time becomes a critical parameter to reduce the noise. However, the minimum noise acceptable for a quantitative XRR analysis depends on a number of analytical situations, including but not limited to

— the base purpose of the XRR experiment (i.e. quality control versus fundamental scientific research),

— the complexity of the sample (i.e. ideal uniform single layer versus complex multi-material thin film stack),

— the intensity of the available X-ray source (i.e. laboratory sealed X-ray tube versus synchrotron source), and

— the time available for the experiment (i.e. high throughput environment versus long-term research environment).

Because this International Standard cannot account for all potential situations, no quantitative guidance regarding a minimum acceptable noise for a specific experiment can be given. However, users should recognize that a reduction in noise by increased count time and/or X-ray intensity will increase the ultimate reliability of any XRR structural determination.

4.8 Detectors

For most instrumental set-ups using laboratory X-ray sources, counting detectors (based e.g. on NaI scintillators) are used. For sources with high intensity (e.g. synchrotron radiation), semiconductor photodiodes can be employed in the photovoltaic mode. The dark current needs to be low (<1 pA) and constant. All remarks in this document referring to count rates do not apply to these detectors.

4.9 Environment

Care shall be taken of the environment in which the data collection is performed. The general, conservative principle to adopt is that no external source shall vary while data are collected during an entire measured scan. Examples of the most common external sources are temperature, humidity, pressure, atmosphere (e.g. gas) and vibrations. Vibrations should be suppressed. A possible solution is to fit the instrument on an anti-vibration base or, alternatively, to hold the beam optics, goniometer and detector arm on a heavy, stable, hard supporting base.

4.10 Data storage

4.10.1 Data output format

It is a common practice, followed by instrument manufacturers, that the collected data are displayed in real time in a graph mode on a display monitor and, at the end of the scan, are saved and stored in the computer controlling the instrument.

Despite the proprietary format of data usually used by manufacturers, whenever possible, it is recommended to save the data according to ASCII code, in two columns, where one column reports the angular position (ω or equivalently 2θ or, equivalently, the scattering vector component q_z) of the collected point and the other column reports the number of counts detected at the same angular position.

4.10.2 Headers

A heading section, clearly separated by the collected data section, is recommended to be included in the stored file. Normally this section is included at the beginning of the stored file, above the collected data

section. The heading section shall include the scans parameters and conditions required for the data analysis and the report.

5 Data analysis

5.1 Preliminary data treatment

The quality and reliability of the final fit result is highly dependent on the quality of the input data.

Before starting to fit data, some treatment of raw data is recommended.

a) Scatter should be subtracted initially for inverse data analysis methods (also called model-independent). For model-dependent data fitting, it can be subtracted prior to fitting, or can be a variable in the fitting process. The description of scatter can include all or some of the contributing factors (constant background, diffuse scatter).

b) Intensity normalization: Normalize intensity by dividing the intensity at each data point by the full beam intensity.

c) Instrument function (including the influence of the resolution of the beam conditioning on the scattering from the specimen). There are two limiting cases:

   1) an empirical curve (such as a Gaussian or pseudo-Voigt function) is convolved with the data at each data point; and

   2) a full analytical description of the beam profile is convolved with the data at each data point.

d) Geometrical correction for the illuminated specimen area (beam footprint, specimen size).

e) Bragg diffraction peaks arising from crystallographic structures shall be either subtracted, or this area of the scan shall be avoided in the XRR data fitting.

5.2 Specimen modelling

5.2.1 General

There are two alternative approaches for XRR data analysis: a) model-dependent (trial-and-error fitting), and b) model-independent (solution of the inversion problem with phase retrieval).

a) The model dependent approach starts with a lamellar description of a physical structure. Each lamella has associated physical parameters (thickness, density, interface width).

b) The model-independent approach reconstructs the electron density profile from the detected reflected X-ray intensity by retrieving the phase of the scattered X-ray waves. There is no *a priori* knowledge or assumption of the specimen structure.

A model-dependent approach is recommended, where it is known that the model is valid, since this approach can give reliable results. If the model is not correct, the results are then, of course, unreliable. This is used in this International Standard; the model-independent approach is not discussed further.

The starting model for the specimen should be the nominal model based on *a priori* physical information (growth conditions, known materials present, other methods, contamination and oxidation especially at the surface). Further development of the model may make it more complex. We recommend that the model is kept to the simplest, physically meaningful workable model to provide an acceptable fit. The data shall be of sufficient quality to justify any complexity of the model.

When a specimen has multiple layers, it may be reasonable to link some fit parameters between some layers by a functional relationship. This reduces the number of free parameters in the fit.

5.2.2 Interface width models

Real interfaces have roughness, i.e. perpendicular deviations of the interface coordinate from the mean surface. In general, two classes of surface roughness[1] can be distinguished:

a) a weak surface waviness extending over several hundreds of nanometres with small inclinations to the average surface (Figure 5);

b) a microscopic surface roughness ranging from atomic length scales to a few nanometres with large inclinations with respect to the average surface (Figure 5). The cut-off wavelength between waviness and roughness is the correlation length of the X-ray reflection (ISO 25178-2).

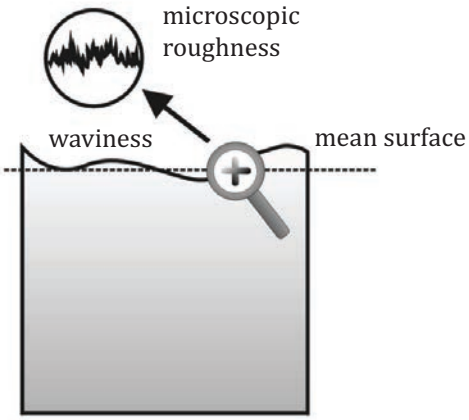

Figure 5 — Waviness and microscopic roughness

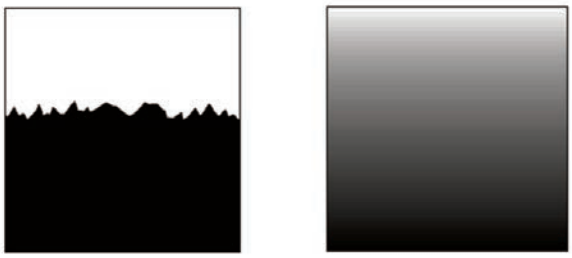

Figure 6 — Roughness and grading of a surface

Figure 6 illustrates the difference between a rough interface with a locally sharp refractive index profile and a graded interface with a smooth refractive index profile. The latter can occur due to intermixing of materials. Both the roughness and the grading lead to a change in the refractive index normal to the interface.[1]

Roughness and interface grading each cause the specular XRR to decrease faster than in the ideal case. Specular XRR cannot distinguish between interface roughness and grading. Since roughness causes the intensity to be scattered in off-specular directions while interface grading does not, diffuse scattering (beyond the scope of this document) can be used to separate the two contributions.

There are several roughness or interface width models used in the literature. The choice of the model depends on the interface roughness character expected for the specimen investigated. Within modelling, it is possible to have an interface width apparently greater than the layer thickness. This may not seem physically reasonable but does constitute a reasonable density profile. In this case, care must be taken

in interpreting the reported fit result in a physically reasonable manner. More detailed analysis of such specimens benefits from measuring diffuse reflectivity.

The abrupt interface model is recommended for statistically non-correlated roughness with a root-mean-square σ. The effect of the abrupt interface can be taken into account by Debye-Waller or Nevot-Croce factors.[1][2]

For specimens with graded interfaces, the model of a transition layer is recommended for essentially correlated roughness and for rms roughness which approximately equals the L_{abs}/θ_c where L_{abs} is an absorption length and θ_c is a critical angle of total external reflection. This interface width can be modelled by analytical functions such as tan, linear, erf, sin, exp. For very large rms roughness values (typically above 5 nm, $\sigma > > L_{abs}/\theta_c$), special models should be applied.[3]

5.3 Simulation of XRR data

There are two basic approaches to simulating X-ray scattering processes from the specimen: kinematic and dynamical theories.[1][2] Dynamical theory is recommended as it gives the more complete description of the process. X-Ray reflectivity simulation software is generally available from commercial vendors of X-ray measurement equipment and from groups such as the synchrotron user community. Information, and, in some cases, downloads are generally available from the associated websites.[1)]

5.4 General examples

Some simulated specular reflectivity data using dynamical theory are shown below to illustrate the effects on the data of different parameters of the sample. Unless otherwise noted, an ideal system is considered in Figures 7 to 12.

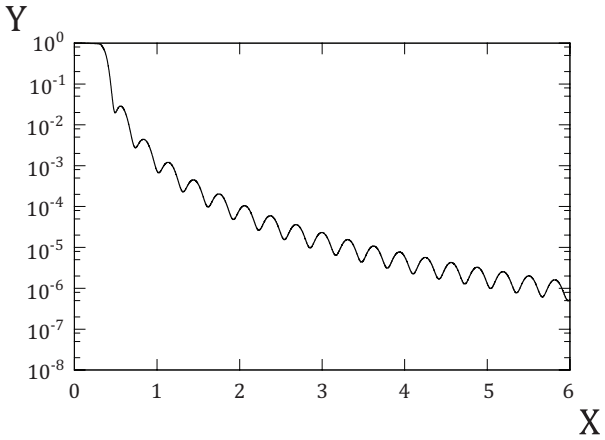

Key

X q_Z, in nm^{-1}

Y intensity, in a.u.

— 20 nm Si_3N_4 layer on Si

NOTE Data may be presented against q_Z, as above, or in angular units. It is also common to normalize the reflected intensity, as shown.

Figure 7 — Simulated specular reflectivity data of a perfectly smooth 20,0 nm Si_3N_4 layer on a perfectly smooth bulk Si substrate

1) Sourceforge is an example of an internet-based source of freely-distributed software. This information is given for the convenience of the users of this document and does not constitute an endorsement by ISO of this product.

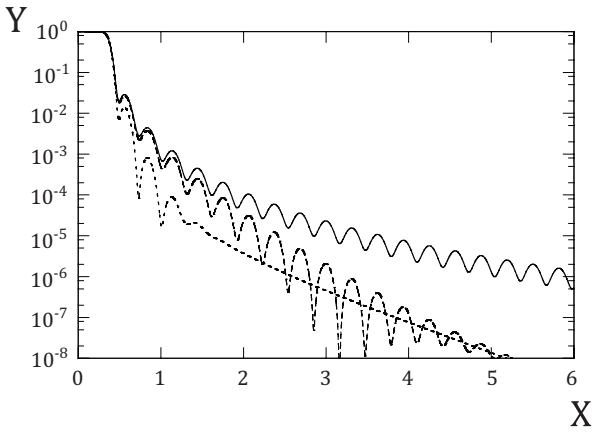

Key

X q_Z, in nm^{-1}
Y intensity, in a.u.

— perfectly smooth Si_3N_4 layer
–– Si_{iw} = 0,3 nm; top_{iw} = 0,6 nm
--- Si_{iw} = 0,3 nm; top_{iw} = 0,2 nm

NOTE Greater interface widths or roughness cause a more rapid decrease in reflected intensity as the specimen angle increases.

Figure 8 — Simulated specular reflectivity data (as in Figure 7) with interface widths of 0,3 nm on the Si surface versus 0,3 nm or 0,6 nm on the top surface

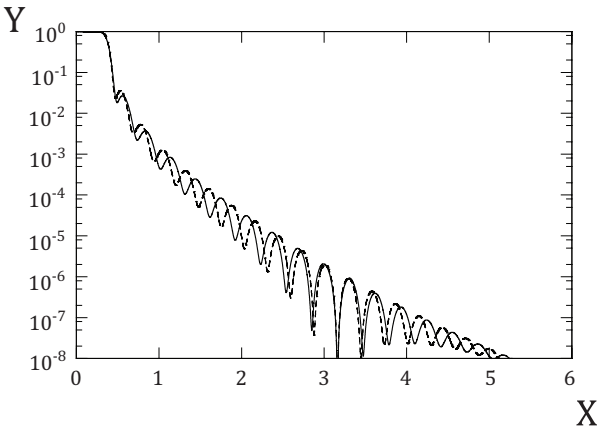

Key

X q_Z, in nm^{-1}
Y intensity, in a.u.

— thickness = 20,0 nm
--- thickness = 22,0 nm

NOTE Thicker layers give narrower fringes in angular space.

Figure 9 — Simulated specular reflectivity of 20,0 nm and 22,0 nm Si_3N_4 (with 0,6 nm surface roughness) on bulk Si (with 0,3 nm interface width)

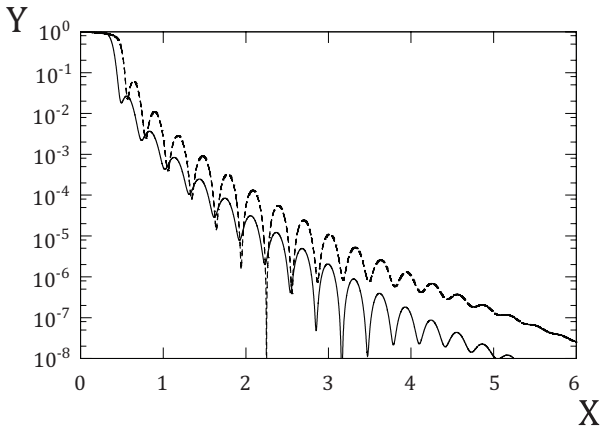

Key

X q_Z, in nm^{-1}
Y intensity, in a.u.
— 20,0 nm Si_3N_4
--- 20,0 nm TiN

NOTE In both cases, there is a 0,3 nm interface width on the Si substrate, and a 0,6 nm roughness on the top surface. TiN is more dense than Si_3N_4, so the critical angle is higher and the fringe contrast is greater.

Figure 10 — Comparison of simulated specular reflectivity for 20,0 nm Si_3N_4 layer and 20,0 nm TiN layer

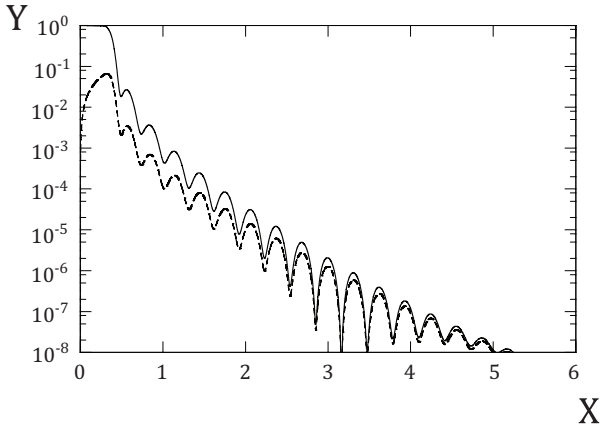

Key

X q_Z, in nm^{-1}
Y intensity, in a.u.
— simulated specular reflectivity of 20,0 nm Si_3N_4 with 0,6 nm surface roughness on bulk SI (with 0,3 nm interface width), without instrument function
--- simulated specular reflectivity of 20,0 nm Si_3N_4 with 0,6 nm surface roughness on bulk SI (with 0,3 nm interface width), with an instrument function (0,5 mm source and detector slits and a 10 mm specimen)

NOTE The position of the critical angle for the small sample is unclear and possibly apparently shifted, and the rate of decrease of reflected intensity with increasing specimen angle is affected, which affects the roughness or interface width deduced if the instrument function is not accurately taken into account in analysis. The positions of fringes are unaffected, so thickness analysis may proceed successfully.

Figure 11 — Comparison of simulated specular reflectivity with and without instrument function

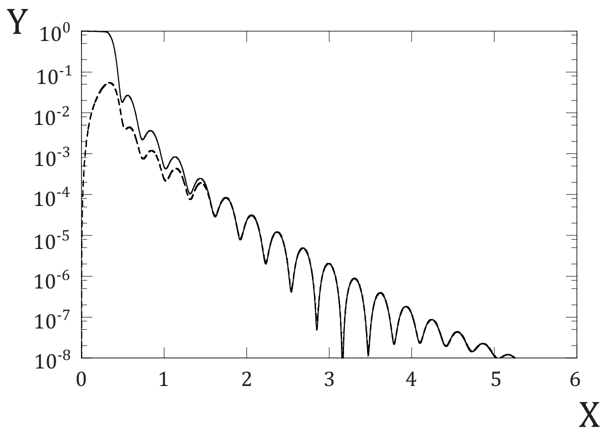

Key

X q_Z, in nm^{-1}

Y intensity, in a.u.

— perfectly flat specimen and ideal incident beam

-- 50 m radius of curvature of the specimen

NOTE The effect also depends on instrument function.

Figure 12 — Effect of 50 m radius of curvature of the specimen on the reflectivity data, compared to a perfectly flat specimen and ideal incident beam

5.5 Data fitting

Data fitting is a trial-and-error technique whereby repeated simulations are compared with the data in order to converge on a best-fit model. Different functions may be selected as a measure of the goodness-of-fit. An initial specimen model is used to simulate an XRR curve (Figure 13). This is compared with the experimental data to calculate a measure of the difference between the simulation and the data. The model is then refined by changing layer (or lamella) (density, interface width, thickness) and external parameters (intensity, background) re-simulated and compared again. This process is repeated until the exit criteria are met (acceptable goodness-of-fit, maximum allowed number of iterations, acceptable tolerance of the improvement of the goodness-of-fit).

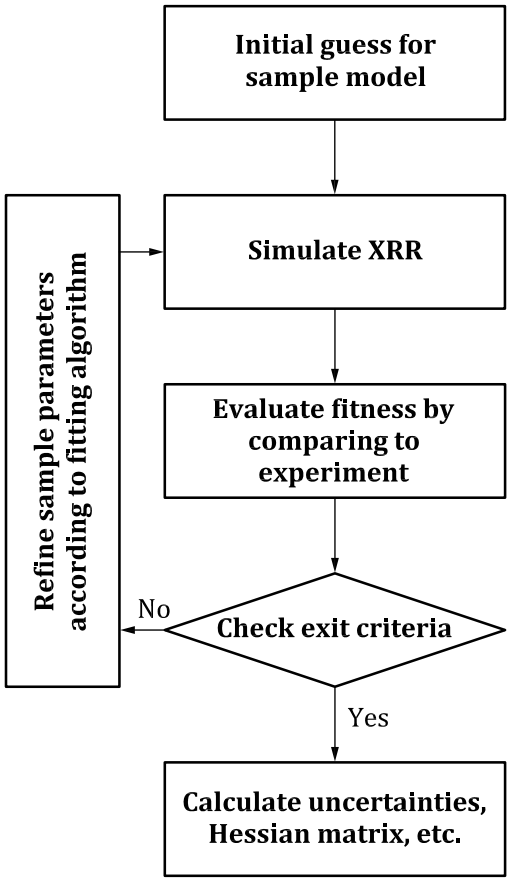

Figure 13 — Data-fitting flow chart

In the model of the specimen, some physical parameters can be selected as fit parameters and some can be fixed. When substrate density or other parameters are known, it is recommended that they be fixed. The fit parameters are allowed to vary within bounds during the fitting process. The initial lower and upper bounds are selected as physically reasonable limits based on the nominal structure. It is recommended that, in most cases, initial bounds are set 10 % to 30 % from the nominal values. Where more accurate information is available *a priori*, narrower bounds can be set. Larger bounds may be needed where initial information is less reliable. The normalizing factor and the variables describing the incoherent scattering can be fit parameters in addition to the specimen structure parameters.

If a good fit is not obtained, it may be necessary to adjust the starting model and/or bounds, and refit.

There are numerous approaches whereby models can be refined. The complete description of all the advanced procedures (both proprietary and non-proprietary) developed in order to get faster fits and achieve robust solutions in complex cases is beyond the scope of this document.

Generally, since the most sensitive parameters in XRR are layer thicknesses, a commonly used approach consist in fitting first layer thicknesses where its initial estimates are obtained from period of thickness oscillations Δq as $2\pi/\Delta q$ if possible. The roughness and layer density parameters are fixed at first. After certain good agreement fitting roughness and density individually or combined can be performed. Which parameter to fix and which one to release strongly depends on the fitting model used. It is usually best to fit the layer densities at the end when the roughness and thicknesses are very close to the final result. In some cases, when the layer density is completely unknown, fitting the layer densities first using some predefined, sometimes equidistant, interfaces of layers is preferable. Layer thicknesses are fixed at the beginning and refined after the densities fitted. If the fitting model is composed from periodical superlattices, it is recommended to fit the thickness period and ratio of thicknesses. If the system has different individual layers, it is usually appropriate to fit individual thicknesses first with roughness and densities fixed.

The fitting process is terminated depending on pre-defined criteria. Without previous experience, it is recommended to continue the fitting process until the goodness-of-fit value is stable and no longer improves with many hundreds of further iterations. Other possible criteria include a defined number of iterations being completed or the best-fit model being stable.

Statistical errors and uncertainties arising on the final fit parameters from the fit process are calculated using the Hessian matrix. Systematic and instrumental errors are not included in this. The diagonal terms of this matrix deliver the standard deviations of the fitted parameters, which reflect their precision. The non-diagonal terms indicate possible correlations between the fitted parameters which relates to the reliability of the specimen model. For example, the roughness of a thin layer may be correlated to its thickness. Errors and uncertainties on the final fit parameters are often delivered by software used for data fitting and they should be stated as combined variance including correlation coefficients from Hessian matrix and a coverage factor giving a proper confidence interval for every fitted value. It is strongly recommended to express the uncertainty for every fitted value in compliance with the *Guide to the expression of uncertainty in measurement*.[13]

The systematic errors depend strongly on good model chosen and sample quality. However if the model is reasonably correct, for good samples, the thickness error is usually not higher than several per cent, see References [11] and [12].

For optimization of the goodness-of-fit function, there are many algorithms available. For example, Genetic Algorithms, Simulated Annealing, Levenberg-Marquardt, Simplex. They can be divided into two classes: The Simplex and the Levenberg-Marquardt methods are the local minimizers, while the Simulated Annealing and Genetic Algorithm are able to find a global minimum of an optimization problem. A comprehensive introduction to the basics of the different optimization methods is given in References [4], [5] and [6]. Reviews of details of these algorithms can be found in, for example, References [7], [8], [9] and [10]. It may be appropriate to combine more than one algorithm sequentially in order to converge on the best fit. It may also be appropriate to try more than one algorithm independently and to compare results.

Where dynamical theory is used for fitting the data, the quality and reliability of the final fit result depends primarily on the quality of the input data.

6 Information required when reporting XRR analysis

6.1 General

As a general rule, any scientific report should contain all the information that is necessary to reproduce the experiment. Thus, a complete report of an XRR analysis should contain appropriate description of the instrument and the experimental details. Since the modelling and fitting process of XRR data are not straightforward, the same consideration applies for the simulation and fitting process. An example of a report is given in Annex A.

6.2 Experimental details

When reporting on XRR experiments, it is important to include the following experimental details:

a) X-ray radiation wavelength (usually the wavelength in nm or Å is reported, in the case of synchrotron radiation the photon energy in eV or keV is more frequently reported);

b) X-ray source size and shape;

c) attenuator factors for the radiation used (if applicable);

d) incident full beam intensity and detector background (both given in, for example counts s^{-1});

e) details of incident and scattered beam conditioning (monochromator, slits, collimator, and other optics):

   1) identities;

2) distances;

3) slit dimensions;

f) incident beam divergence and cross-section at the specimen position;

g) detector type;

h) specimen details (together with collimating slits, specimen length determines the spill-off angle and should not be neglected when reporting XRR experiment;

i) scan parameters – integration time (specify whether not constant), start, step size, stop, and units

1) if a segmented scan is used, these shall be specified for each segment;

j) other significant experimental details [for instance, environmental conditions (temperature, pressure, humidity) and chambers or heating or cooling stages].

6.3 Analysis (simulation and fitting) procedures

The influence of the fitting of the experimental data on the determination of layer properties is not negligible compared with the experimental factors.[11] Thus a full description of the analysis and fitting procedures is strongly recommended. In particular, the following information is needed for a model-based approach:

a) **Possible treatments applied to raw data**.

b) **Initial model for the layered structure.** The choice of the initial model for the layered structure is of crucial relevance in the determination of the final structure. Any information that was useful for guiding the choice of the starting model should be included in the report. Inputs for the construction of the initial model may come from *a priori* knowledge on specimen fabrication, literature, from specimen analysis by complementary characterization techniques of from model independent analysis on the same XRR data.

c) **Calculation method and fitting algorithm**. The report should briefly specify the calculation approach used and what type of fitting algorithm was employed. If a commercially available or custom made software was employed, it should be indicated in the text.

d) **Fitted and fixed parameters.** Not all the parameters that specify a multilayer stack should necessarily be fitted at the same time. When appropriate, some parameters may be kept fixed to the initial value.

e) **Data range.** The data range over which the fit was performed should be specified.

f) **Number of iterations**.

g) **Model final parameters**. The value of all the parameters determining the structure of the layer stack should be reported. For an N layer stack on a bulk substrate, (3N+1) parameters should be specified: the thickness and density of each layer (2N) and the interface width at each interface (N+1). It is worth noting that the physical parameter that ultimately determines the XRR curve is the electron density profile. The mass density may be derived from the electron density when the chemical composition of the layer is known. Reporting on the mass density is recommended when possible.

h) **Density profile**. It is recommended that a plot of the final fitted density profile (density versus depth) is included in the report.

i) **Statistical uncertainty of fitted parameters.**

j) **Goodness-of-fit.** Parameter used during the fitting process. The value can be used as evidence for the reliability of the result.

As an alternative to an analysis based on structural models, a direct inversion (model-free) technique may be employed. In this case, the details of the method used and the final density profile (mass density or electron density) shall be reported.

6.4 Methods for reporting XRR curves

6.4.1 Independent and dependent variables

It is recommended that XRR scan data are displayed as normalized intensity versus the scattering vector q_z (the unit may be nm^{-1} but more often the unit is $Å^{-1}$). The normalized intensity is usually obtained by dividing the reflected intensity by the direct full beam intensity. This choice allows an accurate accounting of the instrument function. The choice of presenting XRR data versus q_z allows direct comparison of data collected using different incident radiation wavelength.

However, the normalized intensity may also be obtained by dividing the reflected intensity by the maximum value of the measured intensities. In this case, important information on the instrument function may be lost. In addition, the physical significance of the data may be compromised if the measured intensity maximum occurs at an angle that is greater than the critical angle.

The scattering vector may be either corrected for refraction or not but, in any case, this should be indicated in the figure caption. Note that attention must be paid since the q_z vector intervals may not be constant when converted from angular values that are equally spaced.

However, XRR curves are sometimes displayed by plotting the reflected intensity (either normalized or non-normalized) versus either ω or 2θ. It is worth noting that, since the position of X-ray source and detector are symmetrical with respect to the normal to the specimen, these two options are completely equivalent. The angles ω and 2θ should be expressed in SI units of radians, or submultiples (for example, milliradians). Angles are also displayed in degrees or submultiples (for example, arc seconds).

6.4.2 Graphical plotting of XRR data

Since the dynamic range of a typical XRR curve covers several order of magnitude, a logarithmic scale is usually preferred for displaying the reflected intensity (see Figure 14). Sometimes it is useful to multiply the measured reflectivity by q_z^4. In this way, the oscillating part of the curve is enhanced and difference between similar curves are clearer (see Figure 15). The plotting of multiple XRR curves on the same graph usually results in an overlap of the curves that prevents a clear representation. Multiple curves can be plotted by shifting each by a constant amount on the ordinate axis. Since representation is in logarithmic scale this means that reflectance values should be multiplied by constant factors, generally a power of 10 (see Figure 16).

The fitted curve should be represented by a solid line overlapped to experimental data (usually represented by symbols).

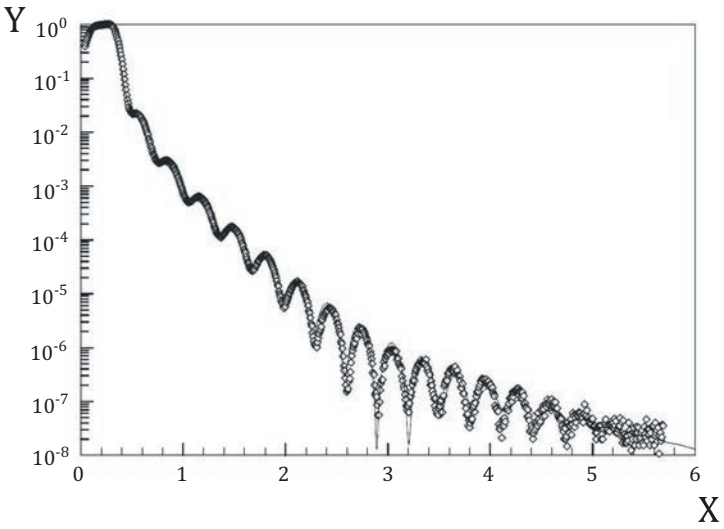

Key

X q_z, in nm^{-1} ◊ experimental data

Y intensity, in a.u. — fit

Figure 14 — Example of experimental and simulated specular reflectivity data of a 20,0 nm Si_3N_4 layer on a Si(100) substrate — Data are presented versus q_z

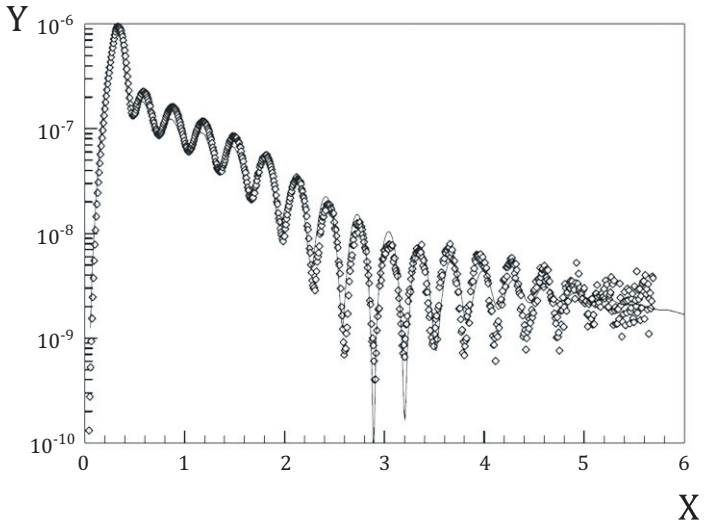

Key

X q_z, in nm^{-1} ◊ experimental data

Y $I \times q_z^4$, in a.u. — best fit

NOTE In this representation, small discrepancies are visible between simulated an experimental data that were not distinguishable in the representation of Figure 14.

Figure 15 — Experimental and simulated specular reflectivity data of a 20,0 nm Si_3N_4 layer on a Si(100) substrate — Intensity multiplied by q_z^4 is plotted against q_z

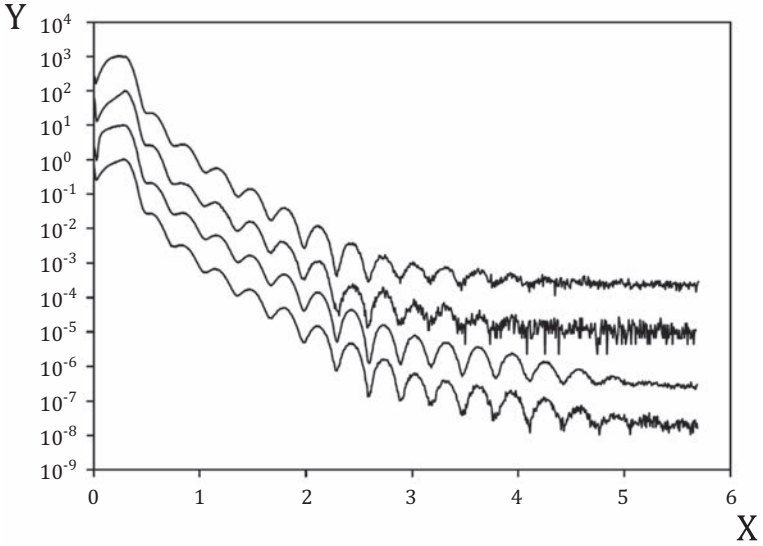

Key

X q_z, in nm^{-1}

Y intensity, in a.u.

NOTE The four curves refer to four different experiments and each is shifted by an order of magnitude on the ordinate scale to improve plot readability.

Figure 16 — Experimental specular reflectivity data of a 20,0 nm Si_3N_4 layer on a Si(100) substrate

Annex A
(informative)

Example of report for an oxynitrided silicon wafer

On 3 October 2007 - 10:28:15, the X-ray laboratory performed XRR measurement on Si_3N_4 samples involving a Si_3N_4/SiO_2 bilayer on a Si wafer substrate. The nominal sample structure was one layer of 20 nm Si_3N_4 and one layer of 1 nm SiO_2 on Si.

Experimental details

— The X-ray experimental device consisted of a Cu X-ray tube with a long fine focus 0,04 × 8 mm^2 operated at power 40kV and 30mA.

— The wavelength used was given by $CuK\alpha_1$ line - λ = 0,154 06 nm.

— Additional aluminium filters were placed in between the detector slit and the detector window. The attenuator factors of the filters were sequentially [1,00 – 5,31 – 27,8 – 148] using the low limit = 11 000 cps (cycles per second) and high limit = 80 000 cps of the detector intensity.

— The intensity of the primary beam was 998 000 cps and the background intensity was 1,0 cps.

— The X-ray beam was monochromatized and collimated by parabolic multilayer mirror and by two Ge 220 double crystals afterwards (Bartels monochromator) giving the output beam divergence 0,003°.

The primary beam was confined by slits 0,4 × 8 mm^2 determining rectangular cross-section of the beam.

A detector slit 0,6 × 10 mm^2 was used after the sample before detector.

The primary-beam slit – sample distance was 14 cm and the sample – detector slit distance was 9 cm.

— Due to low beam divergence 0,003 °, the beam width at the sample position was preserved at 0,4 mm and the height was 9 mm.

— The reflected intensity was recorded by scintillation detector with aluminium filters placed on automatically rotated wheel in between detector slit and the detector window.

The specimen size was 41 × 40 mm^2 placed by longer side parallel to the beam. The sample length 41 mm and beam width 0,4 mm determines the beam spill off at position 0,58°.

The specimen was situated vertically in the goniometer. The scattering plane of the experimental device was in the horizontal direction.

— The $\omega - 2\theta$ scan was performed in the ω range from 0° to 4° with a step size of 0,005° and integration time per point 40s was kept constant during the whole data collection. The measured data were normalized to the primary beam intensity during the measurement.

Analysis (simulation and fitting) procedures

The raw measurement data obtained normalized to primary beam intensity are shown in Figure A.1.

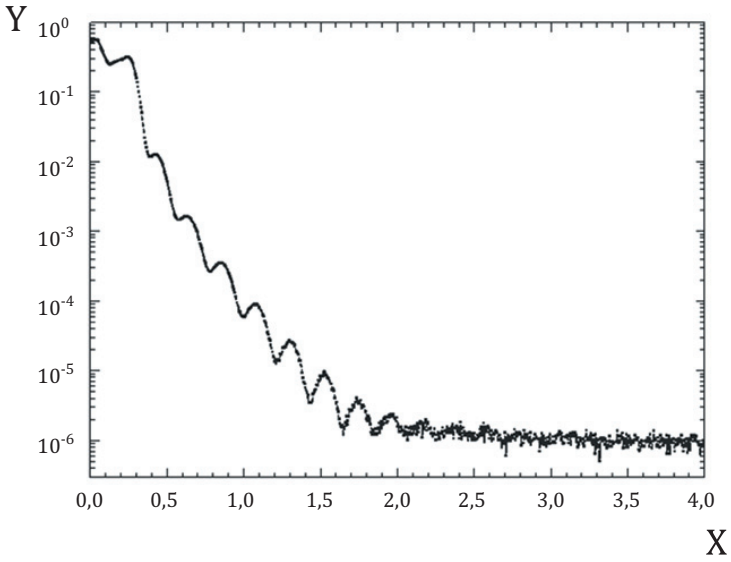

Key

X omega, in degrees — raw measurement data

Y reflectivity

Figure A.1 — Normalized raw data for Si_3N_4 sample 14

Treatment applied to raw data

The raw data were obtained normalized with respect to primary beam and shifted by −0,042° in order to correct small error in omega misalignment.

No subtraction of incoherent signal was necessary due to the low interface roughness or width. The shape of resolution function was also not involved in the analysis since the angular width of resolution function equal to divergence 0,003° is much smaller than the thickness oscillations period.

The influences of background, primary beam and sample spill off for small incidence angles were included in the simulation model.

Initial model

For the simulation and fit, we have used a model involving a Si_3N_4 layer on the top and a SiO_2 layer on the Si substrate. The initial thicknesses of Si_3N_4 and SiO_2 layers were chosen as 19,5 nm and 1,0 nm, respectively. The initial roughnesses or interface widths on top of Si_3N_4 and SiO_2 layers were chosen 0,77 nm and 0,41 nm.

The Si substrate roughness or interface width was fixed to 0,25 nm. The initial density of Si_3N_4 and SiO_2 layers were chosen 2,80 g/cm^3 and 2,20 g/cm^3 respectively and the density of Si substrate was 2,33 g/cm^3.

Calculation method and fitting algorithm

The calculation of the specular XRR data was done by standard matrix optical formalism.[1] Interface roughness or width was included in the model using the decay factor according to Nevot-Croce.[1] The fitting and statistical analysis were performed using Marquart-Levenberg least square fitting algorithm.

For the analysis, we have used fitting software developed in our laboratory.

Fitted and fixed parameters

Both the 2 layer thicknesses and the 2 top interface roughnesses or widths were left free and modified during fitting. The density of the Si_3N_4 layer was also fitted. The densities of SiO_2 and the Si substrate were fixed.

Data range

The fit was performed over the roughness or interface width range from 0,2 nm to 0,9 nm, Si_3N_4 layer thickness range from 10 nm to 30 nm, SiO_2 layer thickness range from 0,5 nm to 2,0 nm and Si_3N_4 layer density range from 2,70 g/cm^3 to 3,29 g/cm^3. The measured data in the range from 0,3° to 3,5° were used only in order to suppress the sample spill off and each data point was fitted using the weight (1/Reflectivity)^{1,5}. The total number of fitted data points was 641.

Number of iterations and final parameters

After 17 iterations, the final parameters shown in Table A.1 were obtained.

Table A.1 — Final data resulting from the fitting

	Roughness or Interface width (nm)		**Thickness** (nm)		**Density** (g/cm^3)	
	average	s.dev.m	average	s.dev.m	average	s.dev.m
Si_3N_4	0,80	± 0,02	19,67	± 0,05	2,87	± 0,14
SiO_2	0,65	± 0,07	0,89	± 0,12	2,20	–
Si	0,25	–	∞		2,32	–

The final residual sum of squares was 26,5. The simulated reflectivity obtained from the final parameters is plotted in the Figure A.2.

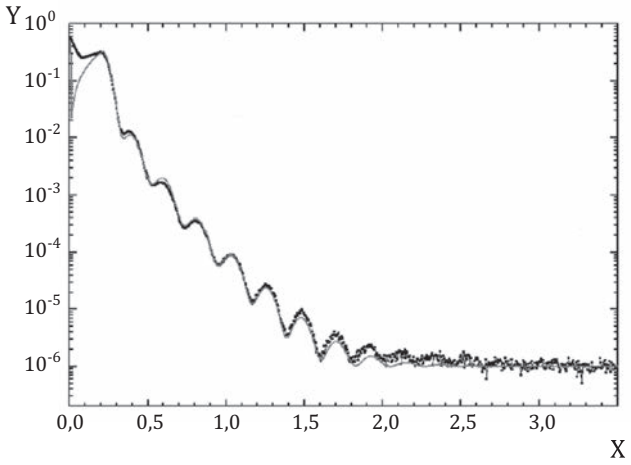

Key

X omega, in degrees
Y reflectivity
■ measurement
— fit

Figure A.2 — Final simulated reflectivity for Si_3N_4 sample 14

Density profile

The density profile simulated according to fitted parameters is shown in Figure A.3.

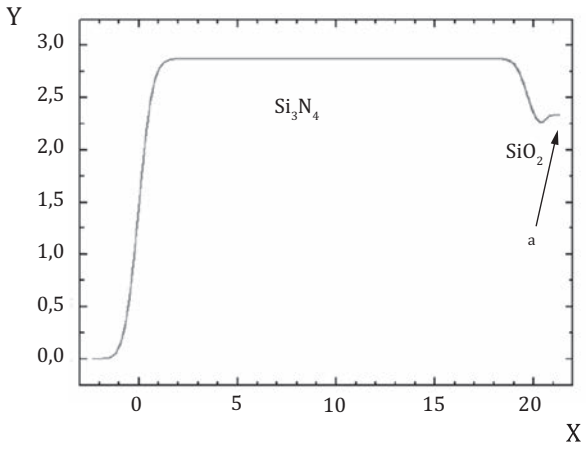

Key

X depth from the surface, in nm
Y density, in g/cm
— density profile simulated from the final fit parameters
a Si substrate

Figure A.3 — Simulated density profile

Bibliography

[1] Pietsch U., Holy V., Baumbach T. *High-resolution X-ray scattering*. Springer, 2004

[2] Daillant J., & Gibaud A.eds. *X-ray and Neutron Reflectivity*. Springer, 2009

[3] Feranchuk I.D., Minkevich A.A., Ulyanenkov A.P. About non-Gaussian behaviour of the Debye-Waller factor at large scattering vectors. *Eur. Phys. J. Appl. Phys.* 2003, **24** p. 21

[4] Ulyanenkov A., Omote K., Harada J. The genetic algorithm: refinement of X-ray reflectivity data from multilayers and thin films. *Physica B*. 2000, **283** p. 237

[5] Ulyanenkov A., & Sobolewski S. Extended genetic algorithm: application to x-ray analysis. *J. Phys. D Appl. Phys.* 2005, **38** p. 235

[6] Wormington M., Panaccione C., Matney K.M., Bowen D.K. Characterization of structures from X-ray scattering data using genetic algorithms. *Philos. Trans. R. Soc. Lond. A.* 1999, **357** pp. 2827–2848

[7] Nelder J.A., & Mead R. A simplex method for function minimization. *Comput. J.* 1965, **7** p. 308

[8] Levenberg K. A method for the solution of certain non-linear problems in least squares. *Q. Appl. Math.* 1944, **2** p. 164

[9] Kirkpatrick S., Gelatt C.D., Vecchi M.P. Optimization by simulated annealing. *Science*. 1983, **220** p. 671

[10] Goldberg D. *Genetic Algorithms in Search, Optimization and Machine Learning*. Addison-Wesley Longman, Bonn, **Vol. 1**, 1989

[11] Colombi P. et al. Reproducibility in X-ray Reflectometry: results from the first world-wide round robin experiment. *J. Appl. Cryst.* 2008, **41** pp. 143–152

[12] Matyi R.J. et al. The International VAMAS Project on X-Ray Reflectivity Measurements for Evaluation of Thin Films and Multilayers – Preliminary Results from the Second Round-Robin. *Thin Solid Films*. 2008, **516** pp. 7962–7966

[13] ISO/IEC Guide 98-3, *Uncertainty of measurement — Part 3: Guide to the expression of uncertainty in measurement (GUM:1995)*

[14] ISO 25178-2, *Geometrical product specifications (GPS) — Surface texture: Areal — Part 2: Terms, definitions and surface texture parameters*

ICS 71.040.40,35.240.70

Price based on 30 pages